INVESTIGATIONS OF THE ELECTRO-OPTICAL PROPERTIES OF MULTICRYSTALLINE SILICON DURING SOLAR CELL PROCESSING

V. Schlosser[1], W. Markowitsch[1], G. Klinger[2], P. Bajons[1], S. Chancy[3], R. Ebner[3], J. Summhammer[3],

1 Institut für Materialphysik der Universität Wien, A-1090 Vienna, Strudlhofgasse 4 (Austria).
Phone: (+43 1) 4277 51428, FAX.: (+43 1) 4277 51429, e-mail: *viktor.schlosser@univie.ac.at*
2 Institut für Meteorologie und Geophysik der Universität Wien, A-1090 Vienna, Althanstaße 14 (Austria).
3 Atominstitut der Österreichischen Universitäten, A-1020 Vienna, Stadionallee 2 (Austria)

ABSTRACT: We used different experimental set ups to detect the optical reflection of free carriers in initial and partly processed multi-crystalline silicon wafer. With these contactless and 'preparation-free' characterization tools we monitored the spatially resolved diffusion length of photoexcited carriers at each step of the solar cell's preparation cycle. A significant change in the distribution of defects was observed. The results are used to (i) improve the steps of solar cell preparation and (ii) to predict an optimized lay out of the front metal grid for each cell depending on its individual defect distribution.
Keywords: Photoelectric Properties, Silicon, Manufacturing and Processing.

1 INTRODUCTION

Crystalline silicon wafers are by far the dominant absorber materials for today's production of solar cells and modules. The advanced production technologies yield in a good price/performance relation. Furthermore silicon exhibit environmental stability and is non-toxic. The wafers are mainly produced either by a solar-optimized Czochralski (Cz)-growth method yielding crystalline silicon with low defect density (c-Si) or by a directional solidification or a ribbon growth method yielding large grained multi-crystalline (mc-Si) wafers with higher defect density [1]. Although the latter manufacturing processes reduce the energy consumption and price per wafer the high defect density causes mc-Si to be an inhomogeneous material with localized regions of high dislocation densities and large impurity and precipitate concentrations acting as carrier recombination sites [2]. Therefore cells of mc-Si most often suffer from a lower conversion efficiency and batches of cells show broader deviations in the solar cell parameter compared to c-Si cells which makes it more difficult to assemble high performance mc-Si modules [3]. The current approach of solar cell manufacturers to minimize these effects is to passivate electrically active defects by the introduction of atomic hydrogen and/or to include a gettering step in the solar cell's preparation procedure. The first process especially is well known to reduce the negative influence of grain boundaries. However due to slow dissolution of precipitates in multi-crystalline Si, metal impurities cannot be effectively removed by conventional P and Al gettering treatments which successfully have been applied to single crystal Si [4]. Recently an other approach to minimize efficiency losses due to grain boundary effects was suggested [5]. The front side metal grid of a mc-Si solar cell is mainly located on the grain boundaries. Two effects were expected to take place. First the shadowing of grains with a high light generated photocurrent density is suppressed. Second it can be assumed that the series resistance is lowered due to a reduction of current paths across grain boundaries. This last method requires the individual identification of the wafer's grain structure in order to evaluate a suitable contact pattern. Although this identification has been done up to now merely by an optical contrast image which do not take into account the electrical activity of the grain boundary an encouraging improvement of the solar cell output supplied with this type of front contact was found [6]. In the present work we report about our in-line investigations of the spatially resolved electro-optical properties of mc-Si during the solar cell processing. The results are intended to be used instead of the optical contrast to evaluate the front contact grid along grain boundaries with respect to electrical inhomogeneities.

The primary objective of mc-Si materials research in photovoltaics is the identification of the dependence of the photoelectric properties of the bulk material on local defects. The lifetime of minority carriers has been widely identified to be the key material parameter determining the conversion efficiency of pn-junction silicon solar cells. Impurities and defects in the crystal lattice reduce the charge carrier lifetime and thus limit the performance of the solar cells. Since the distribution of defects usually varies from grain to grain spatially resolved experiments have to be applied. "Bad grains" with low minority carrier diffusion length generate low open circuit voltage and shunt the "good grains" with high minority carrier diffusion length, thus reducing the overall cell efficiency. It was found that it is more likely to find transition metal clusters in "bad grains" than in "good grains", and that gettering is not efficient in improving the areas of low diffusion length [7]. A variety of techniques were suggested for the investigation of variations of the local minority carrier diffusion length or lifetime – light or electron beam induced photocurrent measurements, scanning photoluminescence, X-ray fluorescence microprobe, X-ray absorption spectromicroscopy, and X-ray beam-induced current – [7,8,9]. Among them the determination of the decay of surface voltage or photocurrent are the most widely used ones. All of the techniques mentioned above require at least some preparation even when they are carried out contactless. For instance a surface passivation for microwave- or optically determined lifetime measurements is needed to accurately separate the bulk properties from surface phenomena. Some of the techniques are time consuming and a complex experimental setup is needed. In order to characterize the photoelectrical properties routinely in-line a solar cell production cycle the measurement should be fast and a special preparation for the measurement must be avoided. Recently Brendel reported about the application of an infrared camera for the analysis of photoexcited charge carrier densities in silicon wafers [10].

2 THEORY

Our intention was to investigate the photoexcited charge carrier distribution in parallel to the processing of the solar cell. Since the measurements should not interfere in any way with the preparation procedure they have to be carried out without electrical wiring and should not require any additional preparation neither change the environmental conditions for the partly processed wafers. The experimental setup should be capable to give sufficient information about the local excess charge distribution in the bulk material with negligible surface related effects. In order to meet the above described requirements completely optically experiments were chosen. The basic idea of all these methods is that a plasma of free charge carriers in any conducting material reflects light below the plasma frequency w_p. The reflection as a function of the wavelength of the incident light depends on the properties of the free carriers. The optical conductivity, s_{opt}, is defined by Equ.1.
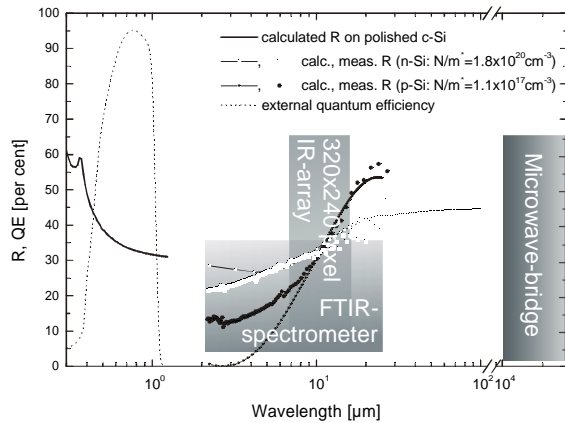
$$s_{opt} = e_0 w_p^2 t = \frac{nq^2}{m_{eff}} t \tag{1}$$

t ... collision time
n ... carrier concentration
q ... elementary charge
m_{eff} ... effective mass
e_0 ... permittivity of free space

$$s_{el} = nq m \tag{2}$$

μ ... carrier mobility

Ideally the electrical conductivity, s_{el}, given by Equ. 2 equals the optical conductivity. Therefore electrical transport properties can be determined from optical measurements. For crystalline silicon s_{opt} agrees with s_{el} very well in most cases. The following three experimental set ups have been used in our experiments. The wavelength range was either in the IR – 2 µm to 25 µm – or in the microwave region – 7500 µm to 37500 µm, or in more convenient frequency units 40 GHz and 8 GHz –. In fig. 1 the measured and calculated reflection of a polished crystalline silicon surface is shown together with the frequency range of our three experiments. For comparison of the wavelength scale a typical quantum efficiency of a crystalline silicon solar cell is plotted.

3 EXPERIMENTAL

3.1 Unprocessed wafer and the base of the solar cell

10 cm × 10 cm mc-Si wafers from Bayer were characterized as delivered with the help of a microwave-bridge. A red laser – λ=635 nm – was focused on the wafer's surface. The backside was placed close to the open end of a waveguide which served as the one end of a bridge circuit. The other branch of the bridge was terminated by an adjustable short. Without illumination of the wafer the bridge was balanced to a minimum output due to destructive interference of the reflected waves from both ends of the bridge. The laser was sinusoidally intensity modulated at a typical frequency of about 10 kHz. The wafers could be moved laterally by the use of a motorized xy-translation table whereas the position of the light beam relative to the open end of the waveguide remained fixed. The frequency and phase locked distortion signal of the microwave-bridge was recorded as a function of the position of the light beam on the wafer's surface. The light beam was focused to less than 50 µm in diameter and its penetration depth in crystalline silicon is below 2 µm. Without fixed charges in or on the wafer the photoexcited carriers which are generated point-like close to the light exposed surface will penetrate due to diffusion into the bulk. Depending on the recombination the carriers experience during their propagation to the back side of the wafer they will alter the amplitude of the detected microwave signal which to a first approximation is proportional to the ratio of the carrier's diffusion length and the wafer thickness, L_n/d. Assuring that the wafer thickness and the incident light intensity is kept constant a plot of the signal versus the position displays a map of the minority carrier diffusion length in the bulk. Principally this detection method equals the well known light beam induced current measurements on contacted solar cells. Therefore it will be
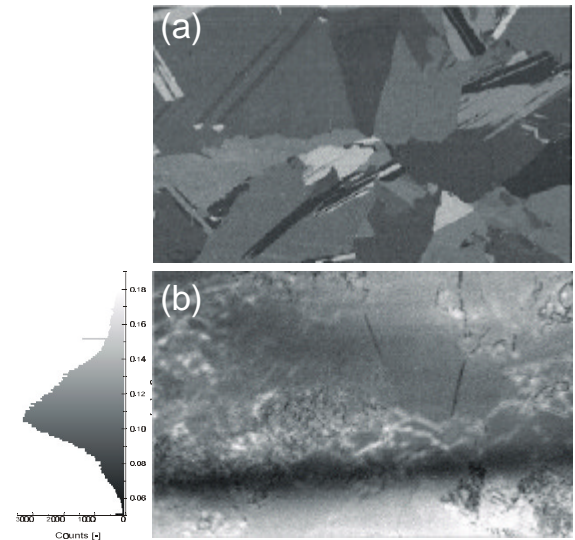

Figure 1: Calculated and measured wavelength dependence of the surface reflection for differently doped c-Si. The accessible wavelength range of our experiments is shown as grey shaded squares.

Figure 2: Optical contrast (a) and microwave detected LBIC (b) image of a 5 cm × 3 cm area of an unprocesses mc-Si wafer.

referred to as microwave detected LBIC – MW-LBIC – further on. Compared to the similar setup for microwave detected lifetime measurements additional contributions arising from surface recombination are sufficiently reduced. This is particularly important for the inspection of the original wafers with a rough surface due to saw damage. Furthermore surface passivation need not to be applied for the measurements. The magnitude of the overall signal level however depends strongly on the surface properties on the side of the wafer which faces the microwave radiation. This makes it difficult to derive absolute values for the minority carrier diffusion length from the measurements. In fig.2 the result of a MW-LBIC scan of a 5 cm × 3 cm area of a wafer as delivered from Bayer is shown. For comparison the optical contrast image of the same area is shown which was obtained with a commercial document scanner. Dark Grey lines indicate grain boundaries with a high concentration of electrically active impurities. Quite often especially these boundaries can not be resolved from the optical contrast because of the small difference of the reflection from the grain's surfaces. Along a part of the grain boundaries an enhancement of the diffusion length as indicated by the light Grey contrast can be seen. We suspect that this is caused by the presence of charged particles which cause a field enhanced diffusion of the photoexcited carriers. These particles potentially were incorporated preferably along grain boundaries during wafer sawing and were removed during the subsequent cleaning and chemical surface preparation. As can be seen in fig.3 which show a MW-LBIC image of the same area of the wafer after these procedures no enhancement of L_n is observed in the vicinity of the previously identified grain boundaries.
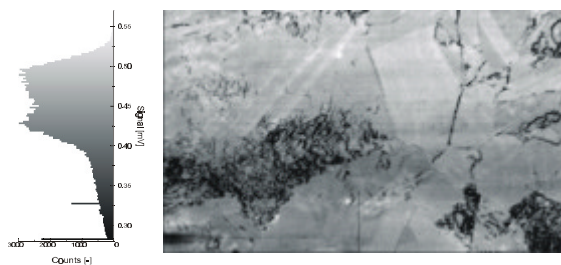
Figure 3: MW-LBIC image mc-Si after cleaning and chemical etching.

Some grains exhibit a high density of dislocations and/or subgrain boundaries as indicated by the dark Grey to Black network of lines. These subgrain defects were not observed on the original wafer and were presumably activated by the chemical polishing.

The emitter was formed by a phosphorous diffusion at 840°C. After this step again the wafer was characterized with the same experimental set up. In this case the emitter was oriented towards the laser beam. Although the drift field introduced by the pn-junction causes a more complex situation for the interpretation of the measured signal qualitatively a comparison of this measurement with the previous experiments still can be done. The MW–LBIC image of the same area investigated before is shown in fig.4. Due to the high temperature process the areas with high crystal defect densities have further spread out. It appears that the length of grain boundaries with undesirable electrical properties was strongly increased compared to the situation after the chemical cleaning and polishing step (fig.3). A potential
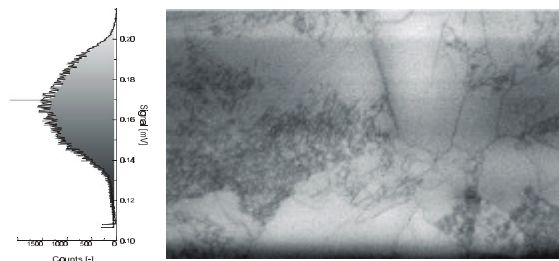
Figure 4: MW-LBIC image of a mc-Si wafer with a highly P doped emitter facing the front surface.

explanation could be that because of the high temperature impurities diffuse out of the grains and accumulate at the grain's surfaces which partly are boundaries to the surrounding grains. As mentioned above the absolute minority carrier diffusion length can not be directly derived from the measured signal. Therefore at the moment we are unable to decide if the diffusion lengths inside the grains have been increased by impurity gettering at the grain boundaries and wafer surfaces during the thermal treatment of the diffusion step. However it is well known that mobile impurities tend to penetrate towards regions with high crystal defect densities.

3.2 The emitter of the solar cell

Due to the observed changes in the distribution of crystal defects and impurities during the emitter formation we carried out further experiments in order to characterize the homogeneity of the shallow highly phosphorous doped layer and to determine its electrical properties. In a first experiment the emitter on a 10 cm × 10 cm wafer with a phosphorous diffused emitter was examined at 9 × 9 positions by a conventional 4 terminal resistance method. The spring contacts were equally spaced in a line and the voltage drop between the two inner electrodes was recorded while keeping the current through the outer electrodes constant. The positioning was motorized and the measurement was fully computer controlled. In a second experiment the reflection at 5 positions – centre and
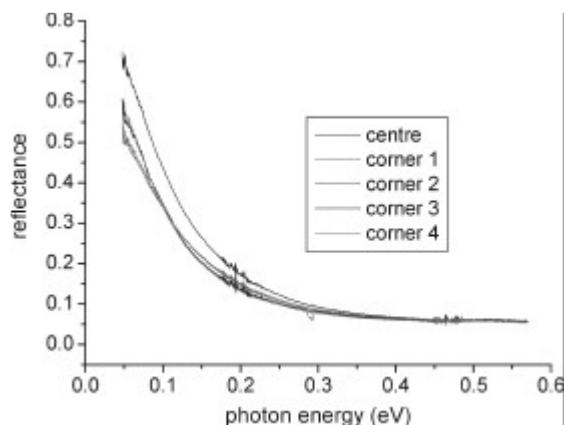
Figure 5: Measured plasma reflectance of a highly doped emitter on mc-Si.

close to the four corners of the wafer – was determined as a function of the wavelength using a JASCO 5300 Fou-

rier transform infrared spectrometer. The light spot on the sample was somewhat less than 1 cm^2 and the wavelength ranged from approximately 2.5 µm to 25 µm (400 cm^{-1} to 4600 cm^{-1}). The obtained spectra in fig.5 show the strong increase of the reflectance towards higher wavelength. The electrical conductivity was derived according to Equ.1 by an extended Drude-Lorentz fit.

In the last experiment we used an Agema 570 thermo camera as parallel operated IR detector array. This device works in the wavelength region from 7 µm to 14 µm and uses a 320×240 focal plane array of bolometers. The camera is capable to produce up to 20 frames/s. The image of an infrared light flash which was reflected by the n-type emitter was recorded. A pulsed light source was used in order to minimize thermal heating of the sample which will additionally be shown in the image. Furthermore a reference image was taken immediately before the light flash was triggered which enables us to subtract thermal contributions to the image arising from the environment. Hence the difference of light exposed and reference image nearly exclusively displays the distribution of the IR light which was reflected from the wafer's surface. Assuring that the wafer is homogeneously illuminated
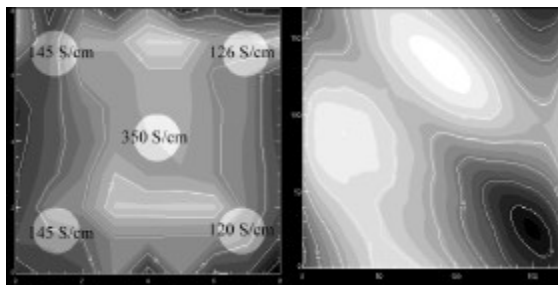
Figure 6: Contour plots of the conductivity of the emitter: Left panel: derived from 9×9 electrical 4 terminal measurements. Right panel: 170×170 pixel image of an reflected IR flash (wavelength 7 µm to 14 µm). At 5 positions (indicated on the left) the reflectance was measured with an FTIR spectrometer

changes in the contrast of the image are caused by local changes in the electrical properties of the free carriers in the emitter. With the experimental set up we currently use these results are close to the resolution of the IR camera. Therefore only a qualitative comparison with the results from the other experiments is shown in fig.6.

4 CONCLUSIONS

An all optical investigation of the properties of free carriers in multi-crystalline silicon wafers and partly processed solar cells was carried out. We have determined the spatially resolved diffusion length of the photoexcited carriers at each step of the solar cell processing sequence. Changes in the distribution of electrically active defects due to processing was logged. Since our experimental set up is contactless and no additional sample preparation has to be done these characterizations do in no way interfere with the manufacturing of the solar cell. Therefore we believe that this is a potential approach to collect routinely in-line information during solar cell manufacturing. Furthermore it offers the opportunity to

handle each wafer individually during processing. Especially the front contact grid can be designed during the processes in such a way that (i) regions with accumulated defects can be excluded which will result in an improved solar cell performance. (ii) For batches of cells the lay out of each front contact grid can be done by interconnecting only selected cell areas such that all devices exhibit an almost unique current voltage characteristics. This simplifies panel assembly and improve its output. To successfully integrate an in-line characterization in an industrial environment the additional time consumption and the labor for each cell has to be minimized. The duration for a complete measurement should be in the order of one second or even less. We began to use a commercial thermocamera with a 320×240 infrared detector array for the detection of the free carrier reflection. Such an array is able to collect the required spatially resolved information in a parallel process in less than 100 ms. The adaptation of the thermocamera for the detection of photoexcited carriers is under progress and is intended to substitute the currently used microwave detected LBIC set up.

REFERENCES

[1] C. Häßler, G. Stollwerk, W. Koch, W. Krumbe, A. Müller, Proc.16th European Photovoltaic Solar Energy Conference (Glasgow, May 2000).

[2] V. G. Popov, Semiconductor Physics Quantum Electronics & Optoelectronics, **3**, (2000) 479.

[3] H. Lautenschlager, F. Lutz, C. Schetter, U. Schubert, R. Schindler, Conference Record of the 26th IEEE Photovoltaic Specialists Conference, IEEE, New York, (1997), 7.

[4] H. Nagel, A. G. Aberle, S. Narayanan, Diffusion and Defect Data Part B Solid State Phenomena, **67-68**, (1999), 503.

[5] J. Summhammer, V. Schlosser, Proceedings of the 12th European Photovoltaic Solar Energy Conference and Exhibition (Amsterdam 1994), H.S.Stephens and Associates (Bedford,UK) 1994, p.734.

[6] R. Ebner, M. Radike, V. Schlosser, J. Summhammer, Proceedings of the 17th European Photovoltaic Solar Energy Conference and Exhibition (Munich, October 2001), WIP Munich (2002), 80.

[7] A. A. Istratova, H. Hieslmair, O. F. Vyvenko, E. R. Weber, R. Schindler, Solar Energy Materials and Solar Cells, **72**, (2002), 441.

[8] S. Ostapenko, I. Tarasov, J. P. Kalejs, C. Haessler, E. U. Reisner, Semiconductor Science and Technology, **15**, (2000), 840.

[9] M. Rinio, H. J. Moller, M. Werner, Diffusion and Defect Data Part B Solid State Phenomena, **63-64**, (1998), 115.

[10] R. Brendel, M. Bail, B. Bodmann, J. Kentschand, M. Schulz, Appl. Phys. Lett., **80**, (2002), 437.